FLEXIBLE SPECTRAL PRECODING FOR SIDELOBE SUPPRESSION IN OFDM SYSTEMS

Khawar Hussain[*] *Ana Lojo*[†] *Roberto López-Valcarce*[*]

[*] atlanTTic Research Center, University of Vigo, Spain. Email: {khawar,valcarce}@gts.uvigo.es
[†] TRedess 2010, S.L., Spain. Email: alojo@tredess.com

ABSTRACT

Spectral precoding is a popular approach to reduce out-of-band radiation (OBR) in multicarrier systems in order to avoid adjacent channel interference. Since precoding will introduce signal distortion, appropriate decoding is required at the receiver side. We present a novel linear precoder design with flexibility to trade off OBR reduction, precoding/decoding complexity, and error rate at the receiver. The precoding matrices have low rank, which translates into significant computational savings. In this way, the requirements of different systems can be satisfied with varying complexity levels.

Index Terms— OFDM, spectral precoding, out-of-band radiation, sidelobe suppression

1. INTRODUCTION

With increasing worldwide demand for data, current 4G cellular standards LTE/LTE-Advanced are expected to reach saturation in a matter of years. There is more than ever demand for next-generation (5G) systems to meet the exponential growth in the number of users, as well as the new requirements for different scenarios and user demands. Recently, the Third Generation Partnership Project (3GPP) has agreed on the use of cyclic-prefix based orthogonal frequency division multiplexing (CP-OFDM) for downlink, and CP-OFDM and Discrete Fourier Transform spread OFDM (DFT-s-OFDM) waveforms for the uplink for 5G phase 1 [1]. OFDM is a mature technology with significant advantages: it is spectrally efficient, robust against multipath effects, and well matched to multiple input-multiple output (MIMO) implementation. Nevertheless, it also has several important drawbacks, such as a large peak-to-average power ratio (PAPR) and large spectrum sidelobes, causing high out-of-band radiation (OBR) and therefore large levels of adjacent channel interference. Traditionally, OBR is mitigated by employing relatively large guard bands, which significantly degrades spectral efficiency.

Many approaches to OBR reduction, each with its own advantages and drawbacks, have been proposed besides conventional methods such as guard band insertion, filtering, and pulse shaping [2, 3]. The use of constellation expansion techniques [4] and multiple choice sequences [5] requires the transmission of side information with each OFDM symbol, causing system overhead. Subcarrier weighting [6, 7] and adaptive symbol transition techniques [8] are data dependent, in the sense that they require solving an optimization problem for each OFDM symbol. Active interference cancellation (AIC) methods modulate some reserved cancellation subcarriers with appropriate data-independent linear combinations of the symbols transmitted on data subcarriers [9, 10].

Spectral precoding, first introduced in [11, 12], is a generalization of AIC in which all subcarriers (and not just a few reserved ones) are modulated with linear combinations of data symbols. A number of linear precoder designs have been proposed to reduce OBR according to different criteria, e.g., smoothing the time-domain waveform [13, 14], introducing out-of-band notches [15, 16], contrast energy ratio [17], or other heuristics [18]. However, whereas AIC operation is transparent to the receiver, which merely discards the cancellation subcarriers, the situation is different with spectral precoding, requiring an appropriate decoder at the receiver to avoid symbol error rate degradation. As a consequence, there is a need to trade off OBR reduction, residual error rate, and computational complexity at both the transmitter (precoder) and receiver (decoder). For example, orthogonal precoders [12, 17, 19] provide very high OBR reduction at the expense of high precoding and decoding complexity, and only recently have reduced-complexity implementations been proposed [20]. Moreover, in certain applications some amount of OBR is acceptable as long as it complies to the corresponding spectral emission mask, so that orthogonal precoding need not be the best choice in terms of system resources.

Motivated by the above considerations, we present a spectral precoder design which is flexible enough to allow the aforementioned complexity/performance tradeoffs. It directly minimizes OBR over a given frequency range without the specification of notch frequencies. The amount of distortion on data subcarriers, which determines the complexity of the decoder at the receiver, is controlled through a user-selectable parameter. In addition, the matrices resulting from the proposed design are approximately low-rank, a property which can be exploited to further reduce complexity.

[*] Supported by Agencia Estatal de Investigación (Spain) and the European Regional Development Fund (ERDF) under project WINTER (TEC2016-76409-C2-2-R, BES-2017-080305), and by Xunta de Galicia (Agrupación Estratéxica Consolidada de Galicia accreditation 2016-2019; Red Temática RedTEIC 2017-2018).

2. SIGNAL MODEL

Consider an OFDM system with N subcarriers spaced Δ_f Hz, cyclic prefix of length $N_{\rm cp}$ and rectangular pulse shaping. Following [21], the spectrum of the kth subcarrier is given by $\phi_k(f) = \varphi(f/\Delta_f - k)G(f)$ for $k = 0, \ldots, N-1$, where

$$\varphi(\nu) \triangleq \frac{\sin\left(\frac{\pi(N+N_{\rm cp})\nu}{N}\right)}{\sin\left(\frac{\pi\nu}{N}\right)} \mathrm{e}^{j\pi\frac{(N+N_{\rm cp})\nu}{N}} \tag{1}$$

and $G(f)$ is the frequency response of the D/A interpolation filter, assumed here to be an ideal brickwall lowpass filter with bandwidth equal to half the sampling rate. Let x_k be the sample modulating the k-th subcarrier for a given OFDM symbol, and let $\boldsymbol{x} = [\, x_0 \ \cdots \ x_{N-1} \,]^T$, $\boldsymbol{\phi}(f) = [\, \phi_0(f) \ \cdots \ \phi_{N-1}(f) \,]^T$. The power spectral density (PSD) can be expressed as

$$P_x(f) \approx \mathbb{E}\{|\boldsymbol{x}^H\boldsymbol{\phi}(f)|^2\} = \boldsymbol{\phi}^H(f)\mathbb{E}\{\boldsymbol{x}\boldsymbol{x}^H\}\boldsymbol{\phi}(f), \tag{2}$$

so that OBR is given by the integral of $P_x(f)$ outside the transmission bandwidth.

In the proposed system, $N_{\rm d} \leq N$ subcarriers are allocated for data transmission, whereas the remaining $N_{\rm c} = N - N_{\rm d}$ subcarriers are specifically modulated to aid in OBR reduction (usually $N_{\rm c} \ll N_{\rm d}$). Thus, let $\boldsymbol{S}$ be the $N \times N_{\rm d}$ matrix given by the columns of $\boldsymbol{I}_N$ with indices corresponding to the data subcarriers, and let $\boldsymbol{T}$ comprise the remaining $N_{\rm c}$ columns of $\boldsymbol{I}_N$. Note that $\boldsymbol{S}^H\boldsymbol{S} = \boldsymbol{I}_{N_{\rm d}}$, $\boldsymbol{T}^H\boldsymbol{T} = \boldsymbol{I}_{N_{\rm c}}$ and $\boldsymbol{S}^H\boldsymbol{T} = \boldsymbol{0}$. Now let $\boldsymbol{d}$ be the $N_{\rm d} \times 1$ data vector to be transmitted in the given OFDM symbol, and let $\boldsymbol{G}$ be the $N \times N_{\rm d}$ precoding matrix, so that

$$\boldsymbol{x} = \boldsymbol{G}\boldsymbol{d} = (\boldsymbol{S}\boldsymbol{P} + \boldsymbol{T}\boldsymbol{Q})\boldsymbol{d}, \tag{3}$$

where $\boldsymbol{P} = \boldsymbol{S}^H\boldsymbol{G}$ (size $N_{\rm d} \times N_{\rm d}$) and $\boldsymbol{Q} = \boldsymbol{T}^H\boldsymbol{G}$ (size $N_{\rm c} \times N_{\rm d}$). In general, due to the presence of $\boldsymbol{P}$, the precoding operation introduces distortion in the data subcarriers[1], with the corresponding performance degradation if no countermeasures are adopted at the receiver.

Assuming $\mathbb{E}\{\boldsymbol{d}\} = \boldsymbol{0}$ and $\mathbb{E}\{\boldsymbol{d}\boldsymbol{d}^H\} = \boldsymbol{I}_{N_{\rm d}}$, (2) becomes

$$\begin{aligned} P_x(f) &\approx \boldsymbol{\phi}^H(f)\boldsymbol{G}\mathbb{E}\{\boldsymbol{d}\boldsymbol{d}^H\}\boldsymbol{G}^H\boldsymbol{\phi}(f) \\ &= \mathrm{tr}\{\boldsymbol{G}^H\boldsymbol{\Phi}(f)\boldsymbol{G}\}, \end{aligned} \tag{4}$$

where we have introduced the matrix $\boldsymbol{\Phi}(f) \triangleq \boldsymbol{\phi}(f)\boldsymbol{\phi}^H(f)$. The total transmission power and the OBR are then given by

$$P_{\rm TOT} = \int_{-\infty}^{\infty} \mathrm{tr}\{\boldsymbol{G}^H\boldsymbol{\Phi}(f)\boldsymbol{G}\}\,\mathrm{d}f = \mathrm{tr}\{\boldsymbol{G}^H\boldsymbol{A}_{\rm TOT}\boldsymbol{G}\}, \tag{5}$$

$$P_{\rm OBR} = \int_{\mathcal{B}} \mathrm{tr}\{\boldsymbol{G}^H\boldsymbol{\Phi}(f)\boldsymbol{G}\}\,\mathrm{d}f = \mathrm{tr}\{\boldsymbol{G}^H\boldsymbol{A}_{\rm OBR}\boldsymbol{G}\}, \tag{6}$$

where $\mathcal{B}$ denotes the out-of-band frequency range, and we have introduced the $N \times N$ positive (semi)definite matrices

$$\boldsymbol{A}_{\rm TOT} \triangleq \int_{-\infty}^{\infty} \boldsymbol{\Phi}(f)\,\mathrm{d}f, \qquad \boldsymbol{A}_{\rm OBR} \triangleq \int_{\mathcal{B}} \boldsymbol{\Phi}(f)\,\mathrm{d}f. \tag{7}$$

[1] An exception is AIC, which is a special case of (3) with $\boldsymbol{P} = \boldsymbol{I}_{N_{\rm d}}$.

3. PROPOSED DESIGN

The symbols modulating the data subcarriers are given by $\boldsymbol{S}^H\boldsymbol{x} = \boldsymbol{P}\boldsymbol{d} \neq \boldsymbol{d}$, and to facilitate the task of the receiver, this distortion should be kept small. The Normalized Mean Squared Error (NMSE) is given by

$$\frac{\mathbb{E}\{\|\boldsymbol{P}\boldsymbol{d} - \boldsymbol{d}\|^2\}}{\mathbb{E}\{\|\boldsymbol{d}\|^2\}} = \frac{1}{N_{\rm d}}\|\boldsymbol{P} - \boldsymbol{I}_{N_{\rm d}}\|_F^2, \tag{8}$$

where $\|\cdot\|_F$ denotes the Frobenius norm. We propose to minimize OBR subject to a constraint on the NMSE, together with the usual total power constraint. The resulting optimization problem can be written as

$$\min_{\boldsymbol{P},\boldsymbol{Q}} \ \mathrm{tr}\{\boldsymbol{G}^H\boldsymbol{A}_{\rm OBR}\boldsymbol{G}\} \quad \text{s.to} \begin{cases} \|\boldsymbol{P} - \boldsymbol{I}_{N_{\rm d}}\|_F^2 \leq N_{\rm d}\epsilon \\ \mathrm{tr}\{\boldsymbol{G}^H\boldsymbol{A}_{\rm TOT}\boldsymbol{G}\} \leq P_{\max} \\ \boldsymbol{S}\boldsymbol{P} + \boldsymbol{T}\boldsymbol{Q} = \boldsymbol{G} \end{cases} \tag{9}$$

where $\epsilon \geq 0$ is the maximum allowable value of the NMSE, and $P_{\max}$ is the maximum available power. Problem (9) is a Least Squares (LS) problem with two Quadratic Inequality constraints, or LS2QI. It is a convex problem, and in principle it can be solved using available convex solvers. However, as the number N of system subcarriers increases, this approach becomes impractical due to the large number of variables involved. This issue is of particular importance in dynamic spectrum access systems which reconfigure their transmissions as spectrum availability conditions evolve.

For that reason, we propose an alternative approach based on the fact that LS problems with a single Quadratic Inequality constraint (LSQI) can be solved efficiently by making used of the Generalized Singular Value Decomposition (GSVD) [22, Ch. 12]. The key observations are: (i) if either of the two inequality constraints is neglected in (9), an LSQI problem results, and (ii) the first inequality constraint in (9) involves $\boldsymbol{P}$ but not $\boldsymbol{Q}$. These facts suggest the following iterative scheme. Starting with some guess $\boldsymbol{P}_1$, for $k \geq 1$ do:

$$\begin{aligned} \boldsymbol{Q}_k &= \arg\min_{\boldsymbol{Q}} P_{\rm OBR}(\boldsymbol{P}_k, \boldsymbol{Q}) \\ &\quad \text{s. to} \quad P_{\rm TOT}(\boldsymbol{P}_k, \boldsymbol{Q}) \leq P_{\max}, \end{aligned} \tag{10}$$

$$\begin{aligned} \boldsymbol{P}_{k+1} &= \arg\min_{\boldsymbol{P}} P_{\rm OBR}(\boldsymbol{P}, \boldsymbol{Q}_k) \\ &\quad \text{s. to} \quad \|\boldsymbol{P} - \boldsymbol{I}_{N_{\rm d}}\|_F^2 \leq N_{\rm d}\epsilon, \end{aligned} \tag{11}$$

where $P_{\rm TOT}$ and $P_{\rm OBR}$ are given by (5) and (6), respectively. The iteration can be initialized with $\boldsymbol{P}_1 = \boldsymbol{I}_{N_{\rm d}}$.

Note that the above iteration (10)-(11) produces a sequence $(\boldsymbol{P}_k, \boldsymbol{Q}_k)$ of feasible points for problem (9), and that the sequence of objective values $P_{\rm OBR}(\boldsymbol{P}_k, \boldsymbol{Q}_k)$ is nonincreasing. Since $P_{\rm OBR}$ is bounded below, the sequence $P_{\rm OBR}(\boldsymbol{P}_k, \boldsymbol{Q}_k)$ must be convergent, and since the feasible set is closed, the convergent point must be feasible.

At the receiver, after carrier and timing synchronization, the cyclic prefix is discarded and an N-point FFT is applied.

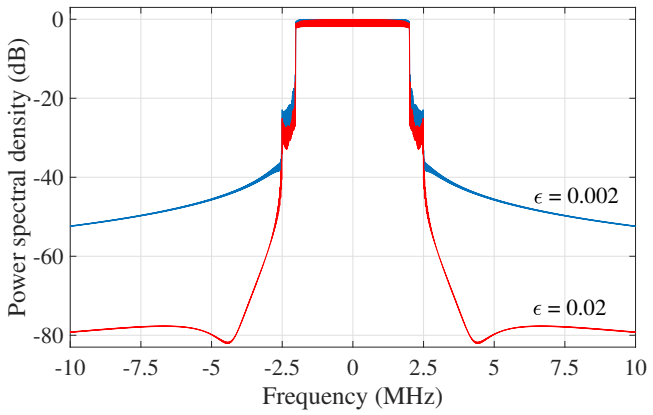

Fig. 1. PSD for different values of ϵ. $N = 256$, $N_{\rm c} = 50$.

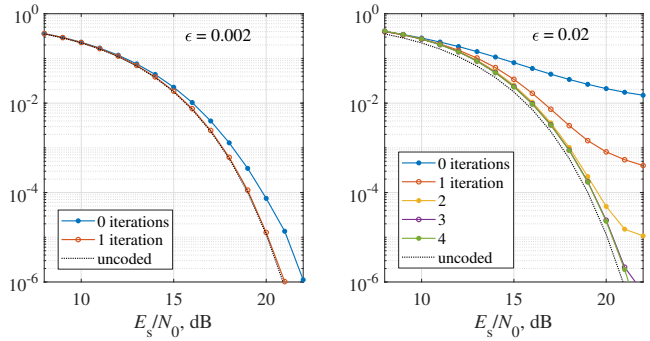

Fig. 2. SER in AWGN channel of the proposed iterative decoder for different values of ϵ. $N = 256$, $N_{\rm c} = 50$.

At its output, the samples corresponding to the $N_{\rm c}$ non-data subcarriers are ignored, and channel equalization is applied to the $N_{\rm d}$ data subcarriers. The resulting $N_{\rm d} \times 1$ vector of samples $\boldsymbol{r}$ can be written as

$$\boldsymbol{r} = \boldsymbol{P}\boldsymbol{d} + \boldsymbol{w} = \boldsymbol{d} + \boldsymbol{\Delta}\boldsymbol{d} + \boldsymbol{w}, \tag{12}$$

where $\boldsymbol{w}$ is the noise vector, and $\boldsymbol{\Delta} \triangleq \boldsymbol{P} - \boldsymbol{I}_{N_{\rm d}}$ is the distortion coefficient, satisfying $\|\boldsymbol{\Delta}\|_F^2 \leq N_{\rm d}\epsilon$ by design. Thus, the fact that this distortion coefficient is small suggests the use of iterative decoding as follows. We initialize $\hat{\boldsymbol{d}}_0 = \boldsymbol{r}$ and, at iteration k, the estimate of the data vector $\boldsymbol{d}$ is obtained as

$$\hat{\boldsymbol{d}}_k = \mathrm{DEC}\{\boldsymbol{r} - \boldsymbol{\Delta}\hat{\boldsymbol{d}}_{k-1}\}, \quad k = 1, 2, \ldots \tag{13}$$

where $\mathrm{DEC}\{\cdot\}$ is an entrywise hard-decision operator, returning for each entry its closest point in the constellation.

4. COMPLEXITY ANALYSIS

Computational complexity plays an important role in energy consumption of limited-power battery-operated devices. The complexity of the proposed design for both the transmitter and receiver, in terms of complex multiplications per OFDM symbol, is discussed below.

4.1. Transmitter Complexity

Direct implementation of the precoder (3) requires $(N_{\rm d} + N_{\rm c})N_{\rm d}$ operations. However, it has been observed empirically that the matrices $\boldsymbol{\Delta}$ and $\boldsymbol{Q}$ are approximately of low rank. Hence, it is possible to truncate their respective SVDs to their $r_\Delta \ll N_{\rm d}$ and $r_Q \ll N_{\rm d}$ principal components, so that they can be accurately approximated as

$$\boldsymbol{\Delta} \approx \boldsymbol{L}_\Delta \boldsymbol{R}_\Delta^H, \qquad \boldsymbol{Q} \approx \boldsymbol{L}_Q \boldsymbol{R}_Q^H, \tag{14}$$

where $\boldsymbol{L}_\Delta$, $\boldsymbol{R}_\Delta$ have size $N_{\rm d} \times r_\Delta$, whereas $\boldsymbol{L}_Q$ and $\boldsymbol{R}_Q$ have size $N_{\rm c} \times r_Q$ and $N_{\rm d} \times r_Q$ respectively. In this way, the transmitter computes $\boldsymbol{P}\boldsymbol{d} \approx \boldsymbol{d} + \boldsymbol{L}_\Delta(\boldsymbol{R}_\Delta^H \boldsymbol{d})$ and $\boldsymbol{Q}\boldsymbol{d} \approx \boldsymbol{L}_Q(\boldsymbol{R}_Q^H \boldsymbol{d})$, requiring $2r_\Delta N_{\rm d} + r_Q(N_{\rm d} + N_{\rm c})$ operations per OFDM symbol. The complexity reduction with respect to direct implementation can be quite significant.

4.2. Receiver Complexity

The computational complexity at the receiver is dominated by the product $\boldsymbol{\Delta}\hat{\boldsymbol{d}}_{k-1}$ in the decoding operation (13). Thus, with direct implementation of such product the total number of operations is $N_{\rm d}^2 N_{\rm it}$, where $N_{\rm it}$ is the total number of decoding iterations. Using the low-rank approximation $\boldsymbol{\Delta} \approx \boldsymbol{L}_\Delta \boldsymbol{R}_\Delta^H$ instead, this number is reduced to $2r_\Delta N_{\rm d} N_{\rm it}$. In practice, $N_{\rm it}$ will depend on the distortion present in the precoded signal: larger values of ϵ will result in improved OBR reduction, but then a larger $N_{\rm it}$ will be likely required.

5. NUMERICAL EXAMPLES

Numerical results are presented next to illustrate the performance of the proposed technique. Power spectral density (PSD) and symbol error rate (SER) are the performance metrics used for comparison. Complexity of the system, which can be a bottleneck for some systems, is also considered.

The proposed technique provides the flexibility to control the trade-off between OBR reduction and system complexity. Fig. 1 shows the PSD obtained with the proposed design for a 5-MHz CP-OFDM system with $1/8$ CP and $N = 256$ subcarriers, of which $N_{\rm d} = 206$ transport 16-QAM data. At the lower and upper spectrum edges, 25 subcarriers are reserved for OBR reduction. The sampling rate of the D/A converter is 20 MHz, so that $\mathcal{B} = [-10, -2.5] \cup [2.5, 10]$ MHz. Clearly, increasing the value of ϵ improves OBR performance, but as shown in Fig. 2 (which considers an AWGN channel), this is at the cost of either SER degradation or increased receiver complexity. With $\epsilon = 0.002$, distortion is small and even without decoding the SER is close to that of an uncoded system; the small gap can be bridged with a single iteration of the proposed decoder. With $\epsilon = 0.02$, OBR is significantly

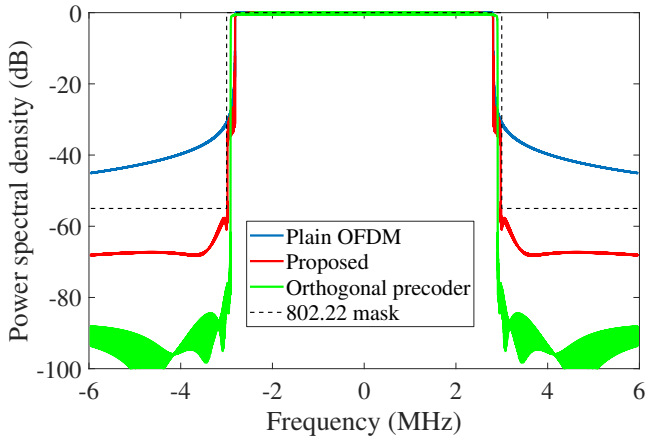

Fig. 3. PSD of different designs and IEEE 802.22 spectral emission mask.

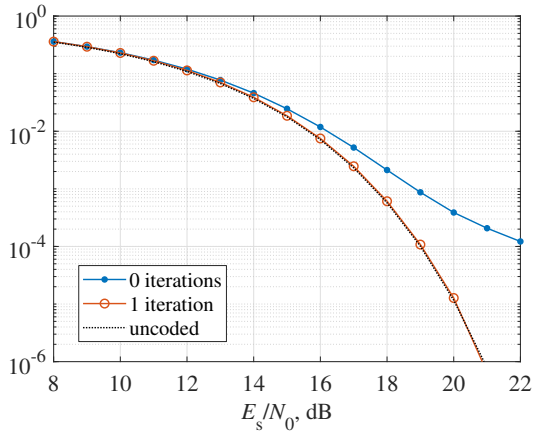

Fig. 4. SER in AWGN channel of the proposed iterative decoder with different number of iterations .

improved (the PSD is reduced by 20 dB at ± 3 MHz form the carrier frequency), but the SER is significantly degraded. Nevertheless, with four decoding iterations the SER is within 0.3 dB of that of the uncoded system.

For performance comparison against other techniques, we have considered the parameters of the IEEE 802.22 standard for 16-QAM transmission in TV White Spaces [23] with 6-MHz TV channels. The system uses $1/32$ CP, subcarrier spacing $\Delta_f = 3.347$ kHz and has a total of $N = 2048$ subcarriers, out of which $N_{\rm d} = 1680$ are used to transmit data. Of the remaining subcarriers, $N_{\rm c} = 100$ are used for active OBR reduction and the rest are turned off.

The proposed design was applied to this setting, taking $\epsilon = 0.002$. The resulting matrices $\boldsymbol{P}$ (size 1680×1680) and $\boldsymbol{Q}$ (size 100×1680) were replaced by their best low-rank approximations with ranks $r_\Delta = 12$ and $r_Q = 10$ respectively, without compromising OBR performance. Fig. 3 shows the resulting PSD together with that of plain OFDM (all non-data subcarriers turned off) and with the orthogonal precoder design from [17]; the IEEE 802.22 spectral emission mask for USA is also shown. It is seen that both precoder designs are mask compliant. Fig. 4 shows the SER of the proposed iterative decoder in an AWGN channel: in this case, the SER of the uncoded case is attained with a single iteration. The SER was also obtained under frequency-selective channels with a number of taps equal to the CP length (64 in this case) and independently Rayleigh fading with exponential power-delay profile. Although not shown here for brevity, it was observed that with a single iteration of the decoder the SER was within 0.05 dB of that of an uncoded system.

The computational load of the proposed design is given in Table 1, together with that of the orthogonal precoder, both with direct implementation and using Clarkson's reduced complexity approach based on Householder reflectors. The complexity of the proposed precoder is only 2% of that of the direct method, and 17% of that of Clarkson's method. Regarding the decoder[2], with a single decoding iteration the figures are 1.3% and 11.6% respectively.

	Orthogonal (direct)	Orthogonal (Clarkson)	Proposed
Transmitter	2,990,400	346,000	58,120
Receiver	2,990,400	346,000	40,320 (1 it.)

Table 1. Computational complexity of different designs (no. of complex multiplications per OFDM symbol).

6. CONCLUSION

We have presented a novel spectral precoder design for multicarrier systems aiming at the reduction of out-of-band radiation. This design provides significant flexibility by adjusting the level of distortion on data subcarriers by means of an user-selectable parameter. The distortion can be compensated at the receiver by iterative decoding, with the number of iterations required for a given error rate typically increasing as more distortion is allowed at the transmitter. In this way a tradeoff between out-of-band radiation and complexity at the receiver can be established. In addition, the resulting precoding matrices have very low rank in practice, which allows for significant computational savings in the on-line implementation of both precoder and decoder.

[2]The precoding matrix $\boldsymbol{G}$ in an orthogonal design has orthonormal columns ($\boldsymbol{G}^H\boldsymbol{G} = \boldsymbol{I}_{N_{\rm d}}$), so the decoding amounts to multipliying the equalized OFDM symbol by $\boldsymbol{G}^H$. This operation does not enhance the noise.

7. REFERENCES

[1] Group Radio Access Network, "TS38.211: NR; Physical channels and modulation (Release 15)," https://portal.3gpp.org/desktopmodules/Specifications/SpecificationDetails.aspx?specificationId=3213, Mar. 2018.

[2] X. Huang, J. A. Zhang, and Y. J. Guo, "Out-of-band emission reduction and a unified framework for precoded OFDM," *IEEE Commun. Mag.*, vol. 53, no. 6, pp. 151–159, Jun. 2015.

[3] M.-F. Tang and B. Su, "Joint window and filter optimization for new waveforms in multicarrier systems," *EURASIP J. Adv. Signal Process.*, vol. 2018, no. 1, pp. 63–82, Oct. 2018.

[4] S. Pagadarai, R. Rajbanshi, A. M. Wyglinski, and G. J. Minden, "Sidelobe suppression for OFDM-based cognitive radios using constellation expansion," in *IEEE Wireless Commun. Netw. Conf.*, 2008, pp. 888–893.

[5] I. Cosovic and V. Janardhanam, "Sidelobe suppression in ofdm systems," in *Multi-Carrier Spread-Spectrum*, Khaled Fazel and Stefan Kaiser, Eds., Dordrecht, 2006, pp. 473–482, Springer Netherlands.

[6] I. Cosovic, S. Brandes, and M. Schnell, "Subcarrier weighting: a method for sidelobe suppression in OFDM systems," *IEEE Commun. Lett.*, vol. 10, no. 6, pp. 444–446, Jun. 2006.

[7] R. Kumar and A. Tyagi, "Extended subcarrier weighting for sidelobe suppression in ofdm based cognitive radio," *Wireless Pers. Commun.*, vol. 87, no. 3, pp. 779–796, Apr. 2016.

[8] H. A. Mahmoud and H. Arslan, "Sidelobe suppression in OFDM-based spectrum sharing systems using adaptive symbol transition," *IEEE Commun. Lett.*, vol. 12, no. 2, pp. 133–135, Feb. 2008.

[9] S. Brandes, I. Cosovic, and M. Schnell, "Reduction of out-of-band radiation in OFDM systems by insertion of cancellation carriers," *IEEE Commun. Lett.*, vol. 10, no. 6, pp. 420–422, Jun. 2006.

[10] J. F. Schmidt, S. Costas-Sanz, and R. López-Valcarce, "Choose your subcarriers wisely: Active interference cancellation for cognitive OFDM," *IEEE J. Emerg. Sel. Topics Circuits Syst.*, vol. 3, no. 4, pp. 615–625, Dec. 2013.

[11] C.-D. Chung, "Correlatively coded OFDM," *IEEE Trans. Wireless Commun.*, vol. 5, no. 8, pp. 2044–2049, Aug. 2006.

[12] C.-D. Chung, "Spectrally precoded OFDM," vol. 54, no. 12, pp. 2173–2185, Dec. 2006.

[13] J. van de Beek and F. Berggren, "N-continuous OFDM," *IEEE Commun. Lett.*, vol. 13, no. 1, pp. 1–3, Jan. 2009.

[14] M. Mohamad, R. Nilsson, and J. van de Beek, "Minimum-EVM N-continuous OFDM," in *IEEE Int. Conf. Commun.*, May 2016, pp. 1–5.

[15] J. van de Beek, "Sculpting the multicarrier spectrum: a novel projection precoder," *IEEE Commun. Lett.*, vol. 13, no. 12, pp. 881–883, Dec. 2009.

[16] J. Zhang, X. Huang, A. Cantoni, and Y. J. Guo, "Sidelobe suppression with orthogonal projection for multicarrier systems," *IEEE Trans. Commun.*, vol. 60, no. 2, pp. 589–599, Feb. 2012.

[17] R. Xu and M. Chen, "A precoding scheme for DFT-based OFDM to suppress sidelobes," *IEEE Commun. Lett.*, vol. 13, no. 10, pp. 776–778, Oct. 2009.

[18] X. Zhou, G. Y. Li, and G. Sun, "Low-complexity spectrum shaping for OFDM-based cognitive radio systems," *IEEE Signal Process. Lett.*, vol. 19, no. 10, pp. 667–670, Oct. 2012.

[19] M. Ma, X. Huang, B. Jiao, and Y. J. Guo, "Optimal orthogonal precoding for power leakage suppression in DFT-based systems," *IEEE Trans. Commun.*, vol. 59, no. 3, pp. 844–853, Mar. 2011.

[20] I. V. L. Clarkson, "Orthogonal precoding for sidelobe suppression in DFT-based systems using block reflectors," in *IEEE Int. Conf. Acoust., Speech, Signal Process.*, 2017, pp. 3709–3713.

[21] T. van Waterschoot, V. Le Nir, J. Duplicy, and M. Moonen, "Analytical expressions for the power spectral density of CP-OFDM and ZP-OFDM signals," *IEEE Signal Process. Lett.*, vol. 17, no. 4, pp. 371–374, Apr. 2010.

[22] G. H. Golub and C. F. Van Loan, *Matrix Computations (3rd Ed.)*, Johns Hopkins University Press, Baltimore, MD, USA, 1996.

[23] IEEE Standard for Wireless Regional Area Networks (WRAN)-Specific Requirements, "Part 22: Cognitive wireless RAN medium access control (MAC) and physical layer (PHY) specifications: Policies and procedures for operation in TV bands," Jul. 2011.